Am J Transl Res 2021;13(4):2181-2197
www.ajtr.org /ISSN:1943-8141/AJTR0115641

Original Article

Circular RNA PCDH10 regulates the tumorigenesis of pancreatic cancer through the miR-338-3p/hTERT axis

Shenfeng Zhang, Meiqing Qiu, Shan Gao, Tao Tian

Department of Oncology, Zaozhuang Municipal Hospital, Zaozhuang 277000, Shandong Province, China

Received June 4, 2020; Accepted December 26, 2020; Epub April 15, 2021; Published April 30, 2021

Abstract: Protocadherin-10 (PCDH10) was previously identified as a pancreatic cancer (PC) suppressor by reducing telomerase activity through binding with human telomerase reverse transcriptase (hTERT). However, we did not observe any effects of PCDH10 on hTERT mRNA or protein expression. Our research found that the PCDH10 gene could be transcribed into linear mRNA or circular RNA, and FUS could bind to the introns flanking the circularized exons, inducing the PCDH10 linear mRNA to shift to circPCDH10 in PC cells. Knockdown of circPCDH10 significantly inhibited PC progression. Mechanistically, circPCDH10 acted as a sponge of miR-338-3p, which could negatively regulate hTERT expression in PC cells. The inhibitory effects of circPCDH10 knockdown on PC cells could be notably reversed by miR-338-3p inhibition and ectopic expression of hTERT. Overall, we propose that the increased FUS expression in PC cells made circPCDH10 the preferred product of the PCDH10 gene, and circPCDH10 might promote PC progression through upregulation of hTERT expression by targeting miR-338-3p.

Keywords: Pancreatic cancer, protocadherin-10, linear, circular, FUS, human telomerase reverse transcriptase

Introduction

Pancreatic cancer (PC), characterized by closely parallel incidence and death rates, is the deadliest malignancies worldwide [1]. To date, surgical resection is the most effective therapeutic strategy for PC patients; however, the recurrence rate of patients who undergo resection remains very high [2, 3]. Consequently, it is urgent to explore the pathogenesis of PC.

Protocadherin 10 (PCDH10) located at chromosome 4q28, was found to be expressed in cancers, including gastric, breast, and colorectal cancer [4-6]. Previous study identified that PCDH10 overexpression can prevent the malignant biological process of PC cells [7, 8]. Meanwhile, research revealed PCDH10 can interact with human telomerase reverse transcriptase (hTERT) to reduce telomerase activity [9]. However, our preliminary experiment discovered that PCDH10 did not reduce the expression of hTERT, but could inhibit telomerase activity, thereby mediating the inhibitory effect of PC phenotype. Based on this, we continue to explore the relationship between PCDH10 and hTERT and its internal mechanism.

Fused in sarcoma (FUS) belongs to the FET (FUS/EWS/TAF15) family [10]. Research confirmed that PUS can involve in the regulation of mRNA synthesis, polyadenylation site selection, intracellular RNA transport, and selective splicing, etc [11]. Studies also demonstrated that FUS was relevant to the development progression of multiple cancers containing prostate cancer [12], cervical cancer [13], thyroid cancer [14], glioma [15], and PC [16] etc. Recently, study verified that FUS can regulate circular RNAs (circRNAs) through introns flanking the splicing junction. Moreover, research testified that various RNA binding proteins (Muscleblind, Quaking, and FUS) can shift the expression of linear mRNAs to circRNAs [17, 18]. However, whether FUS can induce the transfer of PCDH10 linear mRNA to circPCDH10 has not been reported.

CircRNAs are produced in the process of RNA splicing with a closed loop structure [19]. The linear mRNA and circRNAs from the same protein-coding gene can exhibit different functions in regulating biological processes [20]. It is reported that circRNAs have two unique characteristics: more stable than linear transcripts

due to resistance to RNase R, and higher expression than the related linear transcripts [21]. And the main functions of circRNAs consist of functioning as miRNA sponges, regulating transcription, interacting with proteins, and participating in protein translation [22, 23]. CircRNAs are expected to be biomarkers and therapeutic targets for multiple diseases, particularly cancers. Currently, studies have uncovered the critical roles of circRNAs in PC progression [24, 25]. While the related function and mechanism of circPCDH10 in PC are also unclear.

In our study, we certified that the PCDH10 gene could generate circPCDH10 induced by FUS, which had a promotive effect on PC progression by upregulating hTERT expression via the interaction with miR-338-3p. These findings provide a new mechanism by which PCDH10 inhibits PC cell tumorigenesis, which may serve as a new therapeutic target in PC.

Materials and methods

PC samples

We collected PC and corresponding normal tissues from PC patients in *Zaozhuang Municipal Hospital* during the period of 2015-2018. Each PC patient has provided the written informed consent. All protocols have been permitted by the ethics committee of the *Zaozhuang Municipal Hospital*.

Cell lines

The human normal pancreatic cell line HPDE6c7 and 5 PC cells (AsPC-1, BxPC-3, SW1990, PAN-1, PaCa-2) were all purchased from the ATCC (Manassas, USA) and maintained in DMEM including 10% fetal calf serum (FCS, Sigma) at 37°C with 5% CO_2.

Cell transfection

To knock down circPCDH10, three siRNAs against circPCDH10 (si-circPCDH10-1, si-circPCDH10-2, and si-circPCDH10-3) and si-Scramble were synthesized. The three siRNA target sequences were as follows: 1: 5'-CCATATTTGAACTAAACACCA-3'; 2: 5'-CCACCATATTTGAACTAAACA-3'; and 3: 5'-ATTTGAACTAAACACCAGCGA-3'. The cDNAs of circPCDH10 were cloned into the pcDNA3 vector to construct pcDNA-circPCDH10, which was utilized to overexpress circPCDH10 in PaCa-2 and SW1990 cells. MiR-338-3p inhibitors were applied to silence miR-338-3p expression in PC cells. To overexpress hTERT, the cDNAs of hTERT were inserted into the pcDNA3 vector to establish pcDNA3-hTERT. Cells were first placed in DMEM in 6-well plates, then transfected with si-circPCDH10 (50 nM), miR-338-3p inhibitors (100 nM), pcDNA-circPCDH10 (50 ng), or pcDNA-hTERT (50 ng) through Lipofectamine 2000 (Invitrogen).

RT-PCR assay

Total RNAs were obtained by applying TRIzol reagent. NanoDrop2000c (Thermo Scientific, Waltham, USA) was adopted to assess the quality of extracted RNA. After reverse transcription into cDNA, RT-PCR was processed with a SYBR Green PCR Kit (Takara, Otsu, Japan). The data was quantified via the $2^{-\Delta\Delta Ct}$ method and all primer sequences were placed in **Table 1**.

Resistance analysis

First, 2 μg total RNA was disposed of RNase R (4 U/mg, Epicenter Biotechnologies) for 30 min at 37°C. Second, cells were processed with actinomycin D (2 mg/ml, Sigma). Subsequently, gene expression was monitored by qRT-PCR.

CCK-8 assay

After transfecting with corresponding genes, PC cells (5×10^3 cells/well) were subjected to CCK-8 analysis, whereby 10 μL of the CCK-8 solution (Dojindo, Japan) was applied. The absorbance was determined at 450 nm.

Colony formation assay

The PC cells (2×10^4 cells/well) were hatched at 37°C for two weeks in a 6-well plate, then the colonies were calculated following fixation and staining with Giemsa (15 min).

Luciferase reporter assay

We purchased the wild-type (WT) and mutant (Mut) circPCDH10 and hTERT plasmids (named pGL3-circPCDH10-WT, pGL3-circPCDH10-Mut, hTERT-3'UTR-WT and hTERT-3'UTR-Mut plasmids) from Hanbio Company (Shanghai, China). After culture for 16 h, PC cells (1×10^4 cells) were co-transfected with pGL3-circPCDH10-WT (0.5 μg), pGL3-circPCDH10-Mut (0.5 μg), hTERT-3'UTR-WT (0.5 μg), hTERT-

Table 1. The primer sequences in qRT-PCR

Gene	Primer sequences
GAPDH	F: 5'-TATGATGATATCAAGAGGGTAGT-3'
	R: 5'-TGTATCCAAACTCATTGTCATAC-3'
CircPCDH10	F: 5'-ACATCGTGAGCACATTTGAGA-3'
	R: 5'-TCTTGCTGTTCAGGGTGGTA-3'
miR-338-3p	F: 5'-TGCGGTCCAGCATCAGTGAT-3'
	R: 5'-CCAGTGCAGGGTCCGAGGT-3'
hTERT	F: 5'-CGTCCAGACTCCGC TTCATC-3'
	R: 5'-GAGACGCTCGGCCCTCTT-3'
miR-1208	F: 5'-ACACTCCAGCTGGGTCACTGTTCAGACA-3'
	R: 5'-CTCAACTGGTGTCGTGGAGTCGGCAATTCAGTTGAGTCCGCCTG-3'
miR-1231	F: 5'-ACACTCCAGCTGGGGTGTCTGGGCGGAC-3'
	R: 5'-CTCAACTGGTGTCGTGGAGTCGGCAATTCAGTTGAGGCAGCTGT-3'
miR-1253	F: 5'-ACACTCCAGCTGGG-3'
	R: 5'-CTCAACTGGTGTCGTGGAGTCGGCAATTCAGTTGAG-3'
miR-1270	F: 5'-ACACTCCAGCTGGGUGUGUCGAGAAGGTATA-3'
	R: 5'-CTCAACTGGTGTCGTGGAGTCGGCAATTCAGTTGAGgACCTCTA-3'
miR-1299	F: 5'-ACACTCCAGCTGGGTTCTGGAATTCTGTGT-3'
	R: 5'-CTCAACTGGTGTCGTGGAGTCGGCAATTCAGTTGAGTCCCTCAC-3'
miR-1307	F: 5'-ACACTCCAGCTGGGTCGACCGGACCTCGA-3'
	R: 5'-CTCAACTGGTGTCGTGGAGTCGGCAATTCAGTTGAGAGCCGGTC-3'
miR-136	F: 5'-ACACTCCAGCTGGGACTCCATTTGTTTTGAT-3'
	R: 5'-CTCAACTGGTGTCGTGGAGTCGGCAATTCAGTTGAGTCCATCAT-3'
miR-433	F: 5'-ACACTCCAGCTGGGTACGGTGAGCCTGTCA-3'
	R: 5'-CTCAACTGGTGTCGTGGAGTCGGCAATTCAGTTGAGGAATAATG-3'
miR-516b	F: 5'-ACACTCCAGCTGGGATCTGGAGGTAAGAAG-3'
	R: 5'-CTCAACTGGTGTCGTGGAGTCGGCAATTCAGTTGAGAAAGTGCT-3'
miR-524-3p	F: 5'-ACACTCCAGCTGGGGAAGGCGCTTCCCTT-3'
	R: 5'-CTCAACTGGTGTCGTGGAGTCGGCAATTCAGTTGAGACTCCAAA-3'
miR-524-5p	F: 5'-ACACTCCAGCTGGGCTACAAAGGGAAGCAC-3'
	R: 5'-CTCAACTGGTGTCGTGGAGTCGGCAATTCAGTTGAGGAGAAAGT-3'
miR-564	F: 5'-ACACTCCAGCTGGGAGGCACGGTGTCA-3'
	R: 5'-CCAGTCTCAGGGTCCGAGGTATTCGCCTGCTG-3'
miR-607	F: 5'-ACACTCCAGCTGGGGTTCAAATCCAGATC-3'
	R: 5'-CCAGTCTCAGGGTCCGAGGTATTCGTTATAGA-3'
miR-620	F: 5'-ACACTCCAGCTGGGATGGAGATAGATAT-3'
	R: 5'-CCAGTCTCAGGGTCCGAGGTATTCATTTCTAT-3'
miR-634	F: 5'-ACACTCCAGCTGGGAACCAGCACCCCAACT-3'
	R: 5'-CCAGTCTCAGGGTCCGAGGTATTCGTCCAAAG-3'
miR-663b	F: 5'-ACACTCCAGCTGGGGGTGGCCCGGCCGTGC-3'
	R: 5'-CCAGTCTCAGGGTCCGAGGTATTCCCTCAGGC-3'
miR-766	F: 5'-ACACTCCAGCTGGGAGGAGGAATTGGTGCT-3'
	R: 5'-CCAGTCTCAGGGTCCGAGGTATTCAAGACCAG-3'
miR-767-3p	F: 5'-TCTGCTCATACCCCATGGTTTCT-3'
	R: 5'-GTGCAGGGTCCGAGGT-3'
miR-873	F: 5'-ACACTCCAGCTGGGGCAGGAACTTGTGAG-3'
	R: 5'-TCCAGTGCAGGGTCCGAGGT-3'
miR-876-3p	F: 5'-ACACTCCAGCTGGGTGGTGGTTTACAAAGT-3'
	R: 5'-CCAGTCTCAGGGTCCGAGGTATTCTGAATTAC-3'

miR-942	F: 5'-ACACTCCAGCTGGGGTGTACCGGTTTTGTC-3'
	R: 5'-GGTGTCGTGGAGTCG-3'
U6	F: 5'-CGCTTCACGAATTTGCGTGTCAT-3'
	R: 5'-GCTTCGGCAGCACATATACTAAAAT-3'

F, forward; R, revers.

3'UTR-Mut plasmids (0.5 μg) and miR-338-3p mimics (50 nM) or miR-338-3p inhibitors (50 nM). The fluorescence activity was confirmed via Dual-Luciferase Assay System (Promega).

RNA immunoprecipitation (RIP)

RIP was used to explore whether PCDH10 pre-mRNA can interact with the FUS protein via EZMagna RIP kit (Millipore). The putative binding sites of FUS in PCDH10 pre-mRNA were artificially amplified as fragments "a" and "b" by primers. Biotin-labeled a/b fragments were rom Sangon Biotech (Shanghai, China). After lysis, PC cells were addressed with the magnetic beads that recognized biotin overnight at 4°C. Finally, the presence of FUS was confirmed using qRT-PCR. The RIP experiment was conducted using a specific miR-338-3p probe to pull down circPCDH10.

Transwell assay

Transwell chambers (Corning Incorporated, USA) were placed with 20 μl Matrigel matrix (BD Biosciences) in advance for 1 h. Treated PC cells were resuspended and counted using serum-free medium. Then, PC cells in each group (200 μl, 5×10^5 cells/ml) was spread to the upper chambers, and 500 μl medium with 20% FCS was placed to the lower chambers. After 24 h at 37°C, 4% paraformaldehyde was applied to fix the cells, and 0.5% crystal violet was adopted to stain the cells. The invaded PC cells were determined using a microscope.

Wound healing assay

In brief, the processed PC cells were maintained overnight at 37°C. A sterile plastic pipette tip was utilized to create wounds by scratching the cell layer. After washing with PBS, scratched the processed PC cells were maintained for 24 h.

In vivo tumor growth

SW1990 cells transfected with si-circPCDH10 were resuspended in DMEM to a final concentration of 2×10^6 cells/mL. Then, male BALB/c mice (Eight-week-old) were injected with 100 μL of circPCDH10-silenced SW1990 cell suspension at the left flanks. Tumor growth was examined at 10, 15, 20, 25, 30, 35, and 40 days after injection.

Statistical analysis

Data were from 3 independent replicates. The differential analysis was conducted using SPSS with Student's t test. And $P < 0.05$ denoted that the difference is significant.

Results

Characterization and validation of circPCDH10

CircPCDH10 originates from the PCDH10 gene and consists of exons 2-4, while linear PCDH10 mRNA is transcribed from exons 1-5 of the PCDH10 gene (**Figure 1A**). The sequence of the splice junctions of circPCDH10 was examined by Sanger sequencing (**Figure 1B**). We adopted cDNA and gDNA extracted from PC tissues and PaCa-2 and SW1990 cells as templates to amplify the linear PCDH10 mRNA and circPCDH10. We discovered that circPCDH10 could be amplified using divergent primers from the cDNA of PC tissues and cells (**Figure 1C**). RNase R and actinomycin D were used to further validate circPCDH10 in PC cells, and the results indicated that circPCDH10, but not PCDH10 mRNA, was resistant to digestion by RNase R and actinomycin D exonuclease (**$P < 0.01$, **Figure 1D** and **1E**), confirming the circular form of circPCDH10.

FUS bound the introns flanking the circularized exons and negatively regulated circPCDH10 expression in PC cells

By informatic prediction, we found two binding sites of FUS at both ends of PCDH10 pre-mRNA, one upstream and another downstream (**Figure 2A**). The two binding fragments were amplified by primer1 and primer2 and named "a" and "b", respectively (**Figure 2A**). The interaction between PCDH10 pre-mRNA

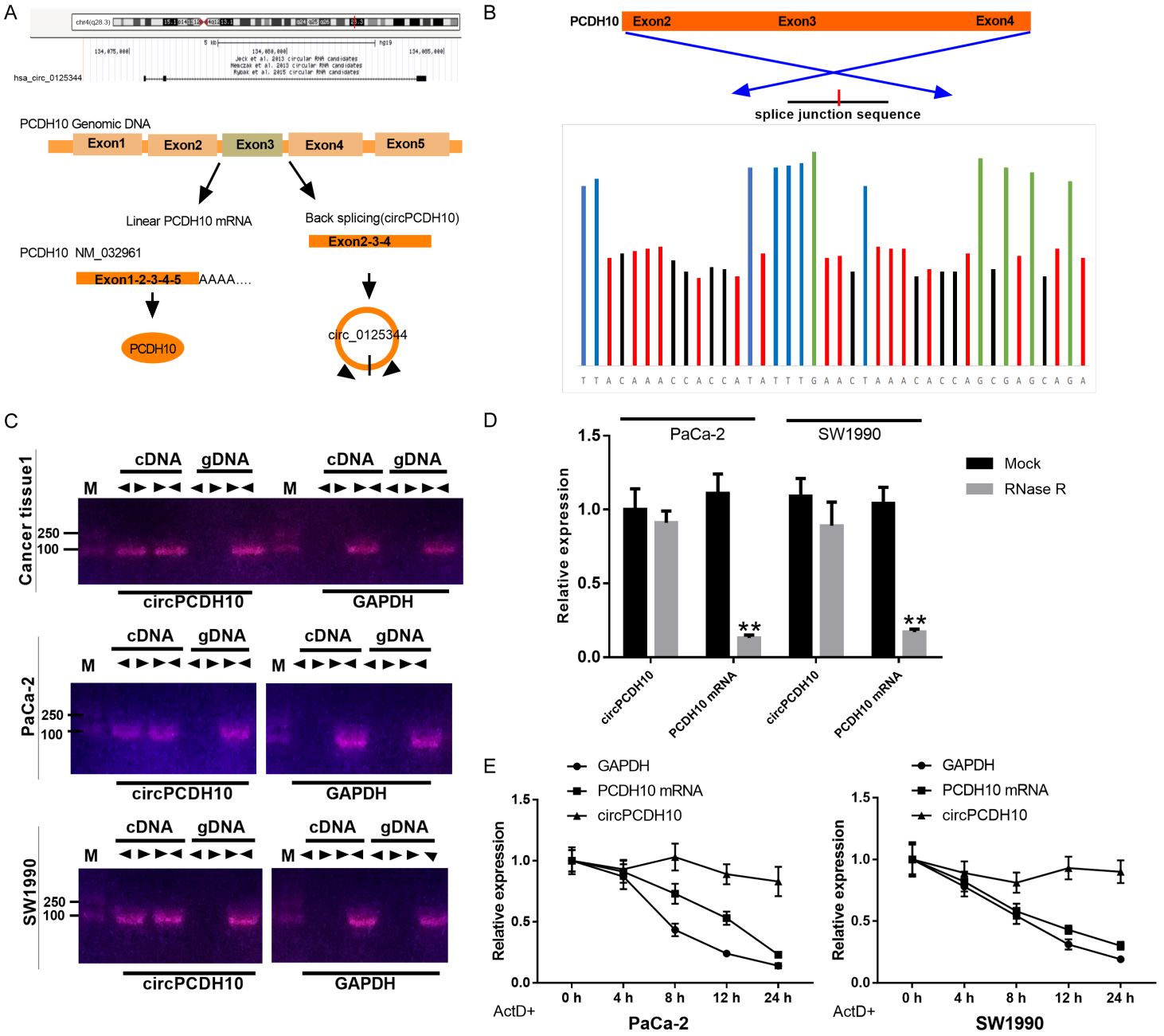
A
hsa_circ_0125344
PCDH10 Genomic DNA
Exon1
Exon2
Exon3
Exon4
Exon5
Linear PCDH10 mRNA
Back splicing(circPCDH10)
Exon2-3-4
PCDH10 NM_032961
Exon1-2-3-4-5
AAAA....
PCDH10
circ_0125344
B
PCDH10
Exon2
Exon3
Exon4
splice junction sequence
T T A C A A A C C A C C A T A T T T G A A C T A A A C A C C A G C G A G C A G A
C
Cancer tissue1
PaCa-2
SW1990
cDNA
gDNA
M
250
100
circPCDH10
GAPDH
D
PaCa-2
SW1990
Mock
RNase R
Relative expression
1.5
1.0
0.5
0.0
**
circPCDH10
PCDH10 mRNA
E
GAPDH
PCDH10 mRNA
circPCDH10
Relative expression
ActD+
0 h
4 h
8 h
12 h
24 h
PaCa-2
SW1990

Figure 1. Characterization and validation of circPCDH10. A. Gene structure of PCDH10 and the schematic diagram of linear and circular PCDH10 RNA formation. B. Sanger sequencing of circPCDH10 in back-splice junctions. C. The linear or circular PCDH10 were amplified using cDNA and gDNA of PC tissues and cell lines. D. qRT-PCR verification of linear and circular PCDH10 in PC cells treated with RNase R. E. qRT-PCR verification of the linear and circular PCDH10 in PC cells treated with actinomycin D. $^{**}P < 0.01$.

A

circRNA	Tag Name	% Identity	Alignment Length	Mismatches	Gap Openings	Tag Start	Tag End	circRNA Start	circRNA ENd	Upstream/Downstream
hsa_circ_0125344	HHMF2_288047_FUS_rep2_9_36	100.00	36	0	0	1	36	-761	-726	Upstream
hsa_circ_0125344	HHMF3_323700_FUS_rep3_10_30	100.00	30	0	0	1	30	+471	+500	Downstream

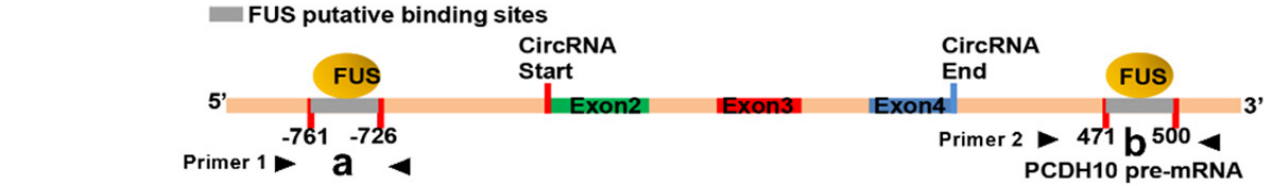

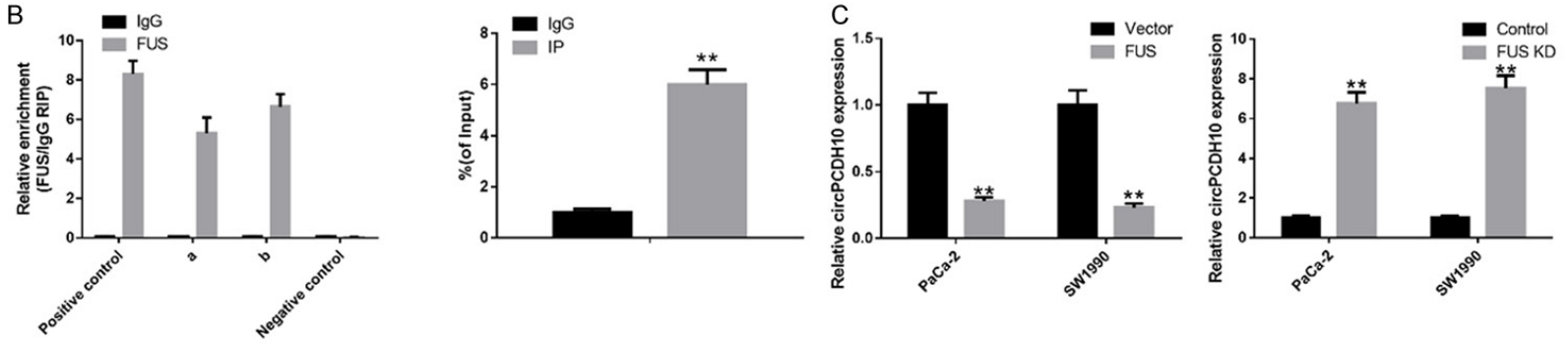

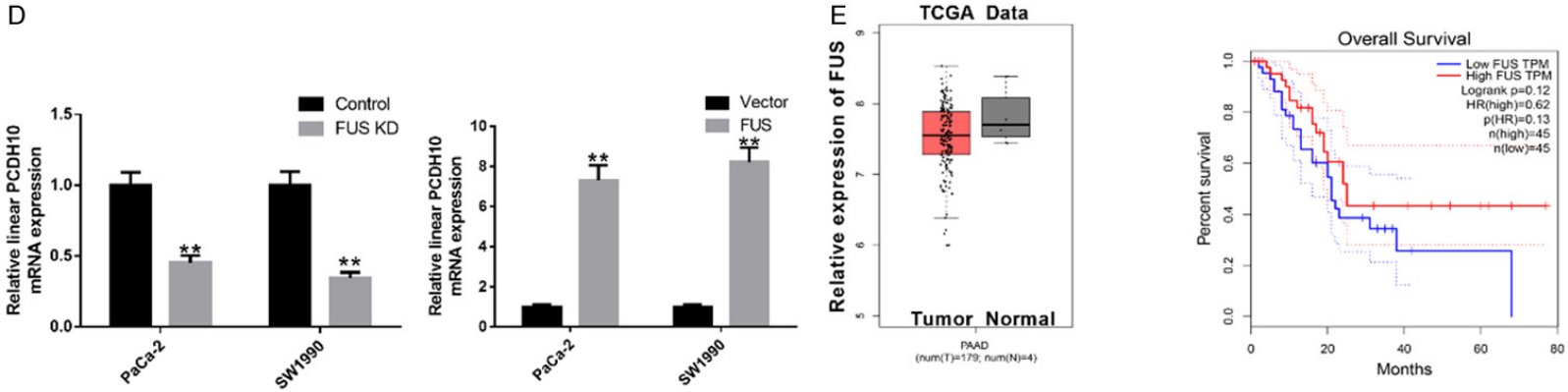

Figure 2. FUS can bind the introns flanking and downregulate circPCDH10 in PC cells. A. The location of two predicted binding sites of FUS in PCDH10 pre-mRNA. B. RIP-qRT-PCR analysis of the interaction between FUS and PCDH10 pre-mRNA. C. Relative circPCDH10 expression in FUS-overexpressing or FUS-silenced PC cells. D. Relative linear PCDH10 expression in FUS-overexpressing or FUS-silenced PC cells. E. Relative expression of FUS from TCGA data and overall survival rate in PC were displayed. $^{**}P < 0.01$.

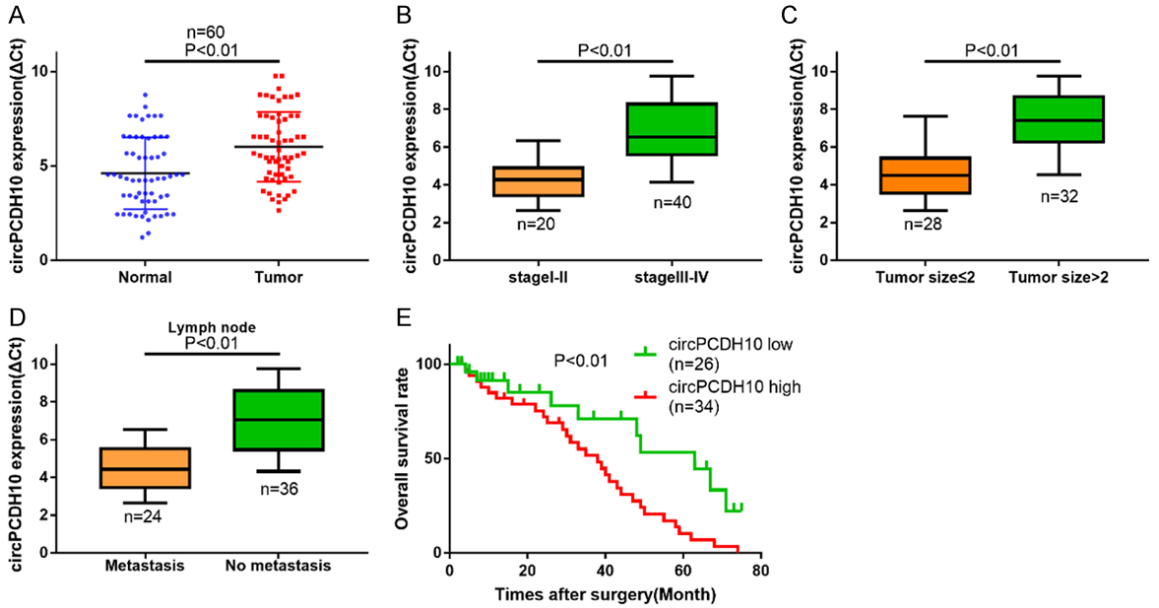

Figure 3. Increased circPCDH10 expression in PC indicated a worse prognosis. A. Relative circPCDH10 expression was examined in normal and PC tissue samples by qRT-PCR analysis. B. CircPCDH10 expression was monitored via qRT-PCR assay in different clinical stages of PC. C. CircPCDH10 expression in PC patients with tumor size less than 2 or greater than 2 was detected through qRT-PC. D. CircPCDH10 expression in PC patients with or without metastasis. E. CircPCDH10-related overall survival rate was certified in PC patients. $^{**}P < 0.01$.

and FUS was confirmed using specific probes of the "a" and "b" fragments. We revealed a specific enrichment of FUS in the positive, "a" and "b", groups but not in the negative group ($P < 0.01$, **Figure 2B**). We then examined circPCDH10 expression in PC cells treated with FUS overexpression or FUS knockdown (KD) by qRT-PCR. The results uncovered that FUS caused a significant downregulation of circPCDH10 in PC cells ($P < 0.01$, **Figure 2C**); however, circPCDH10 expression was significantly upregulated in PC cells after FUS KD treatment ($P < 0.01$, **Figure 2C**). Linear PCDH10 mRNA expression was also measured in FUS KD- and FUS-treated PC cells, and the results announced that linear PCDH10 mRNA expression was distinctly downregulated in FUS KD-treated PC cells ($P < 0.01$, **Figure 2D**), whereas it was significantly upregulated in FUS-treated PC cells ($P < 0.01$, **Figure 2D**). In the TCGA data, we found that FUS expression was remarkably decreased in the PC tumor samples versus normal samples ($P < 0.05$, **Figure 2E**). In addition, we manifested that patients with low FUS expression (N = 45) tended to have a worse survival rate than those with high FUS expression (n = 45), although the $P = 0.12$ (**Figure 2E**).

Increased circPCDH10 expression in PC indicated a worse prognosis

The results from **Figure 2** demonstrated that FUS could negatively regulate circPCDH10 expression, and FUS was reduced in PC, implying that circPCDH10 expression increased in PC. To confirm this hypothesis, we confirmed circPCDH10 expression in PC and corresponding normal tissue samples (n = 60) by qRT-PCR assay. The results showed that circPCDH10 expression was higher in PC tissue samples than that in normal samples ($P < 0.01$, **Figure 3A**). Moreover, we discovered that circPCDH10 expression was positively correlated with the clinical stage (P < 0.01, **Figure 3B**) and tumor size ($P < 0.01$, **Figure 3C**) but negatively corre-

Table 2. Analysis of the relationship between circPCDH10 and clinical characters in PC

Clinicopathologic Characteristics	No. of patients	CircPCDH10		*P* value
		High	Low	
Age (year)				
> 50	31	14 (45.2%)	17(54.8%)	0.380
≤ 50	29	11 (37.9%)	18 (62.1%)	
Gender				
Male	33	18 (54.5%)	15 (45.5%)	0.520
Female	27	14 (51.9%)	13 (48.1%)	
Tumor size (cm)				
< 2	28	10 (35.7%)	18 (64.3%)	0.005**
≥ 2	32	23 (71.9%)	9 (28.1%)	
Differentiation grade				
Well/moderately	35	13 (37.1%)	22 (62.9%)	0.008**
Poorly/undifferentiated	25	18 (72%)	7 (28%)	
Distal metastasis				
M0	24	8 (33.3%)	16 (66.7%)	0.003**
M1	36	26 (72.2%)	10 (27.8%)	
TNM stage				
0 & I & II	20	6 (30.0%)	14 (70.0%)	0.006**
III & IV	40	27 (67.5%)	13 (32.5%)	

**$P < 0.01$.

lated with metastasis ($P < 0.01$, **Figure 3D**). The results also certified that PC patients with high circPCDH10 expression (N = 34) exhibited a worse overall survival rate than those with low circPCDH10 expression (n = 26) ($P < 0.01$, **Figure 3E**). Additionally, the results revealed that circPCDH10 expression was in connection with the tumor size ($P = 0.005$), differentiation grade ($P = 0.008$), distal metastasis ($P = 0.003$), and tumor, node, metastasis (TNM) stage ($P = 0.006$) but was not related to age ($P = 0.380$) or gender ($P = 0.520$, **Table 2**).

Knockdown of circPCDH10 inhibited PC tumor progression

Before we explored its role in PC tumorigenesis, the expression level of circPCDH10 was upregulated in the five PC cell lines relative to the HPDE6c7 cell line ($P < 0.01$, **Figure 4A**). Then, we silenced circPCDH10 expression in PaCa-2 and SW1990 cells by transfecting cells with circPCDH10 siRNAs. The knockdown efficiency of circPCDH10 siRNAs was then assessed in PC cells, and si-circPCDH10-1 showed the best knockdown efficiency ($P < 0.01$, **Figure 4B**). Furthermore, we used si-circPCDH10-1 to block circPCDH10 expression in PC cells, followed by the analysis of PC cells-related functions. PC cells transfected with si-circPCDH10 showed reduced cell viability versus cells transfected with si-Scramble ($P < 0.01$, **Figure 4C**). And the number of colonies in the si-circPCDH10-treated group was significantly reduced versus that in the si-Scramble-treated group ($P < 0.01$, **Figure 4D**). In the *in vivo* tumor growth assay, the results indicated a remarkable downregulation in the si-circPCDH10 group versus the si-Scramble group ($P < 0.01$, **Figure 4E**). The data showed that knockdown of circPCDH10 in PC cells significantly attenuated invasion ($P < 0.01$, **Figure 4F**) and migration ($P < 0.01$, **Figure 4G**). E-cadherin mRNA expression was remarkably increased in circPCDH10-blocked PC cells, while circPCDH10 knockdown resulted in a significant downregulation of N-cadherin mRNA ($P < 0.01$, **Figure 4H**).

circPCDH10 functioned as a sponge of miR-338-3p

To address the distribution of circPCDH10 in PaCa-2 cells, we examined circPCDH10 expression in the cytoplasm and nucleus through qRT-PCR. The data uncovered that that circPCDH10 was located in the cytoplasm of PaCa-2 cells ($P < 0.01$, **Figure 5A**). It is well documented that circRNAs could memorably interact with miRNAs in the cytoplasm. Thus, we particularly predicted the target miRNAs of circPCDH10 by using the online tool CircInteractome and then assessed their expression in circPCDH10-overexpressing PaCa-2 cells. The results announced that circPCDH10 overexpression only downregulated two miRNAs (miR-338-3p and miR-873) in PaCa-2 cells ($P < 0.01$, **Figure 5A**). We then chose miR-338-3p for further study. Subsequently, WT and Mut circPCDH10 fragments (**Figure 5C**) were cloned into the pGL3 vector to generate pGL3-circPCDH10WT and pGL3-PCDH10Mut. We demonstrated that miR-

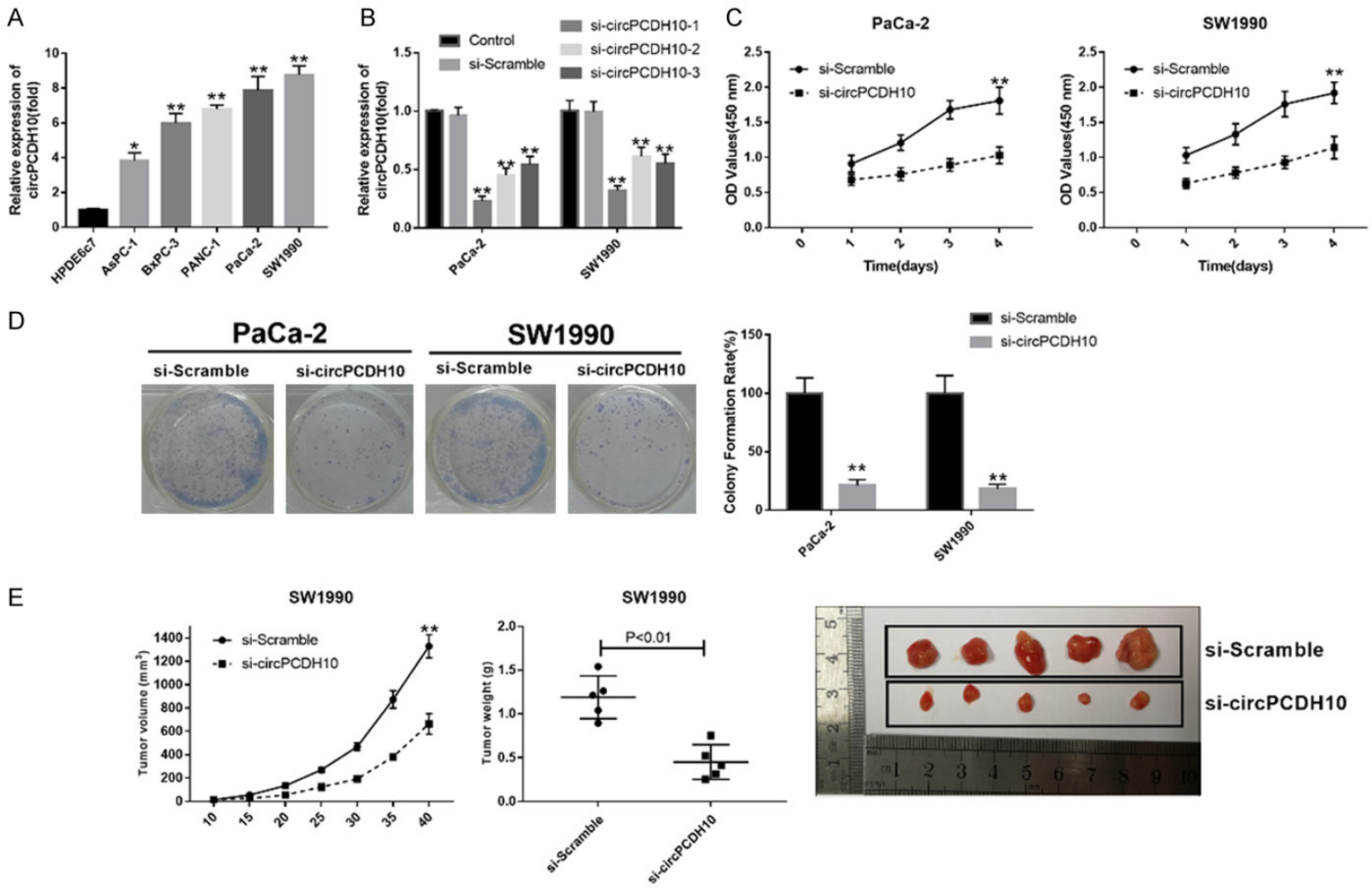
A
Relative expression of circPCDH10(fold)
HPDE6c7
AsPC-1
BxPC-3
PANC-1
PaCa-2
SW1990
B
Control
si-Scramble
si-circPCDH10-1
si-circPCDH10-2
si-circPCDH10-3
Relative expression of circPCDH10(fold)
PaCa-2
SW1990
C
PaCa-2
SW1990
si-Scramble
si-circPCDH10
OD Values(450 nm)
Time(days)
D
PaCa-2
SW1990
si-Scramble
si-circPCDH10
Colony Formation Rate(%)
E
SW1990
si-Scramble
si-circPCDH10
Tumor volume (mm³)
SW1990
P<0.01
Tumor weight (g)
si-Scramble
si-circPCDH10

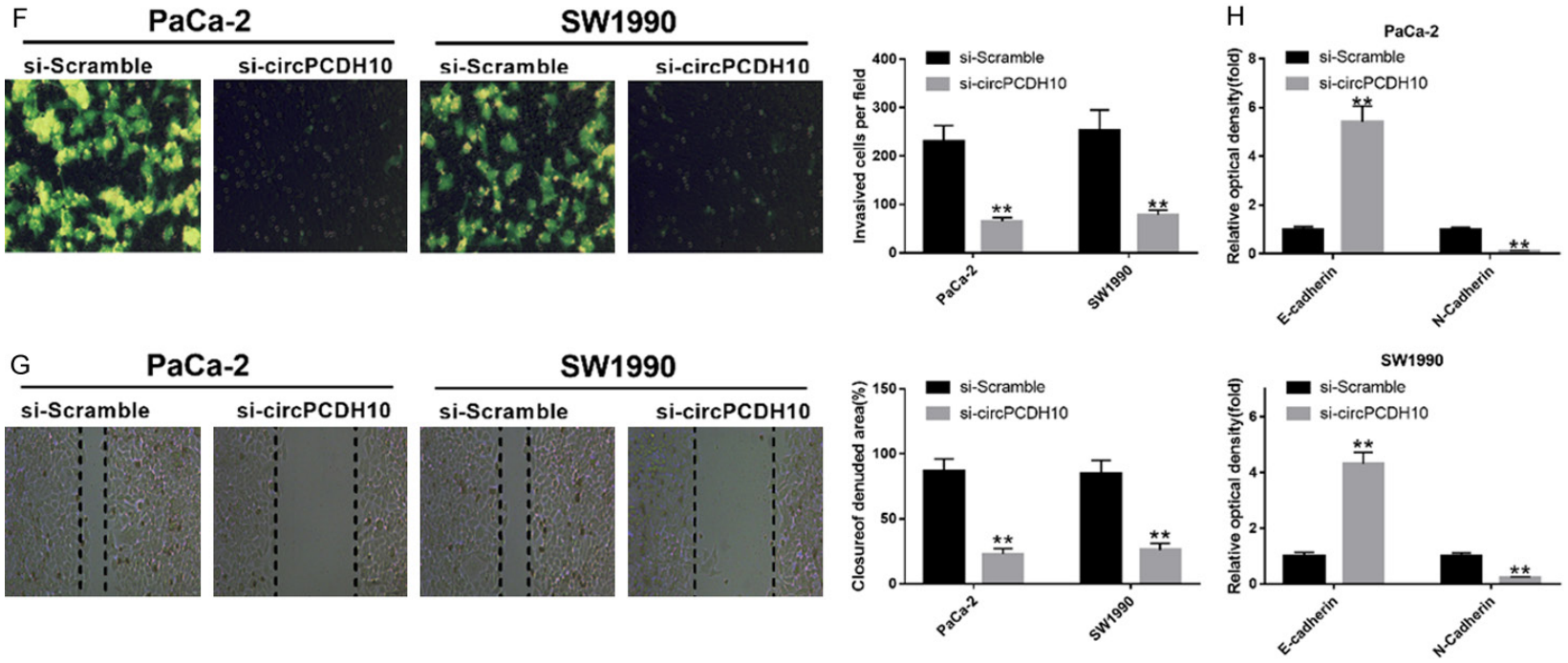

Figure 4. Knockdown of circPCDH10 inhibited PC tumor progression. A. Relative circPCDH10 expression in HPDE6c7 and PC cell lines. B. Relative circPCDH10 expression in PC cells with nothing (control), si-Scramble, or circPCDH10 siRNAs (si-circPCDH10-1~3). C and D. Cell proliferation was assessed in circPCDH10-silenced PC cells. E. SW1990 cells with si-circPCDH10 or si-Scramble were injected into BALB/c nude mice, and tumor volume and weight were evaluated. F. The effects of circPCDH10 knockdown on PC cell invasion were determined by Transwell assay in si-circPCDH10-transfected PC cells. G. A wound healing assay was conducted to analyze the migration of PC cells treated with si-circPCDH10. H. E-cadherin and N-cadherin expressions in si-circPCDH10-transfected PC cells were examined by qRT-PCR. $^{**}P < 0.01$.

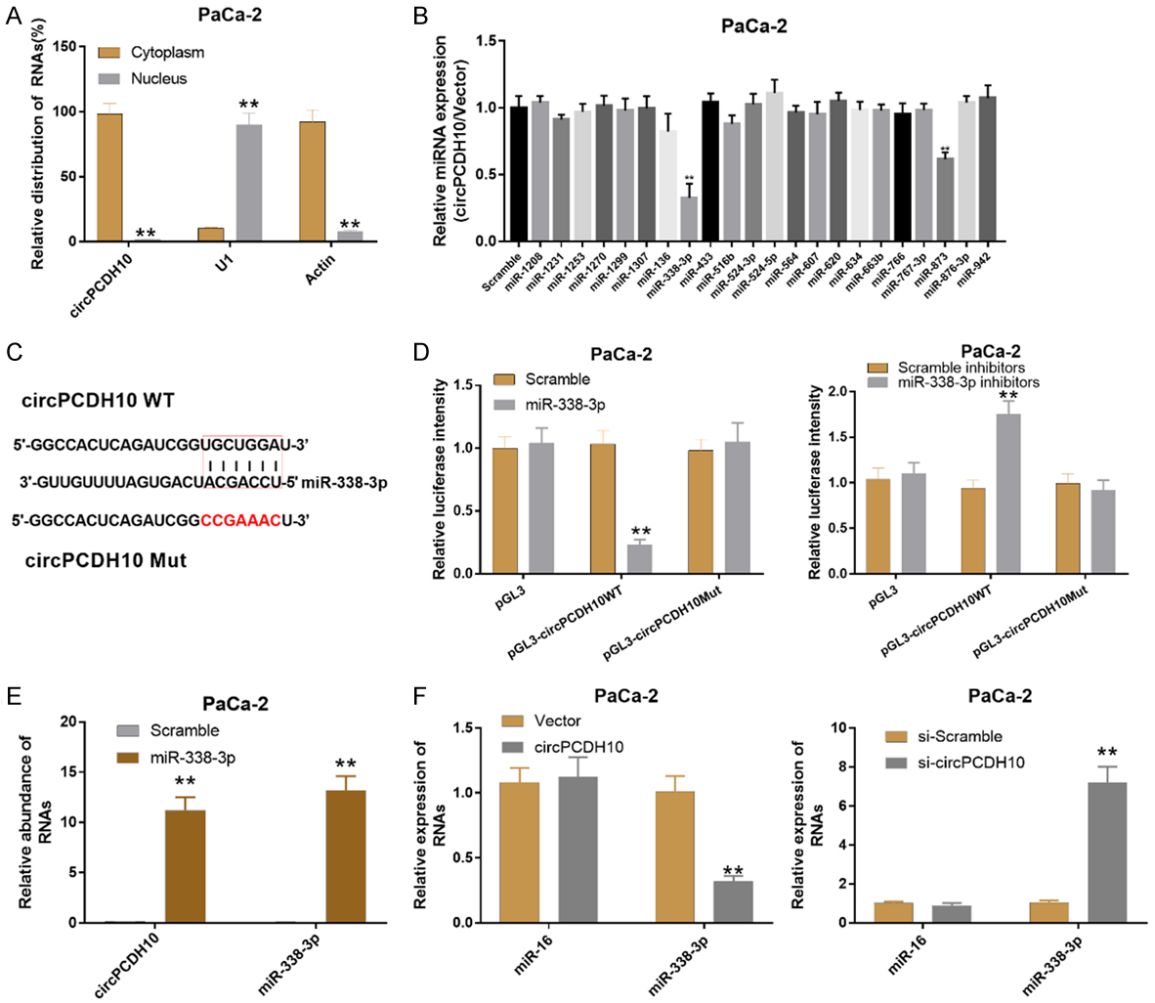

Figure 5. CircPCDH10 targeted miR-338-3p. A. Distribution of circPCDH10 in PaCa-2 cells. B. Relative expression of 22 miRNAs in PaCa-2 cells treated with circPCDH10 or its scramble control. C. The WT and Mut sequences between circPCDH10 and miR-338-3p. D. The relevance of circPCDH10 and miR-338-3p was verified through luciferase reporter assay. E. The identification of RIP assay in PaCa-2 cells. F. miR-338-3p expression was defined through qRT-PCR in circPCDH10-overexpressing or circPCDH10-silenced PaCa-2 cells. $^{**}P < 0.01$.

338-3p could markedly attenuate the luciferase activity in PaCa-2 cells driven by pGL3-circPCDH10WT, and miR-338-3p inhibitors could enhance the luciferase activity in PaCa-2 cells driven by pGL3-circPCDH10WT ($P < 0.01$, **Figure 5D**). The luciferase activity driven by pGL3-PCDH10Mut and pGL3 was not affected by miR-338-3p. RIP assays, followed by qRT-PCR detection, were proceed to further confirm the regulation between miR-338-3p and circPCDH10 in PaCa-2 cells. The results denoted that a specific enrichment of circPCDH10 and miR-338-3p in the miR-338-3p-specific probe group versus the scramble group ($P < 0.01$, **Figure 5E**). In addition, in circPCDH10-overexpressing PaCa-2 cells, miR-338-3p was significantly downregulated, while miR-338-3p expression was remarkably upregulated in circPCDH10-blocked PaCa-2 cells, and miR-16 was used as a negative control ($P < 0.01$, **Figure 5F**).

miR-338-3p downregulated hTERT by targeting binding

To further prove the downstream molecular mechanism of miR-338-3p, we identified the related target genes through five different bioinformatics analysis tools (miRWalk, Microt4, miRMap, RNA22, and TargetScan). A total of 788 target genes were identified, and among them, hTERT attracted the most attention

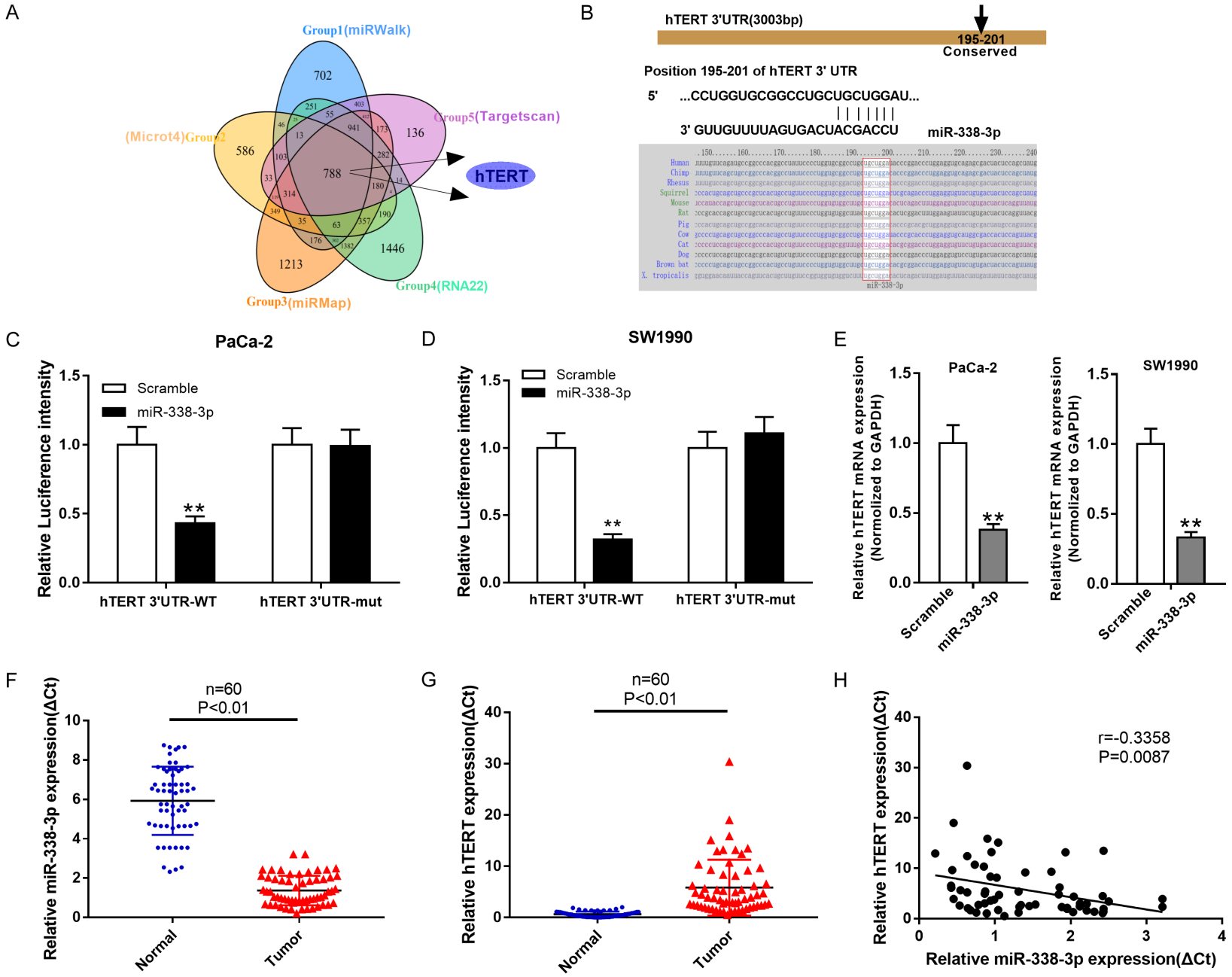
A
Group1(miRWalk)
Group2(Microt4)
Group5(Targetscan)
Group4(RNA22)
Group3(miRMap)
hTERT
B
hTERT 3'UTR(3003bp)
195-201
Conserved
Position 195-201 of hTERT 3' UTR
5' ...CCUGGUGCGGCCUGCUGCUGGAU...
3' GUUGUUUUAGUGACUACGACCU
miR-338-3p
C
PaCa-2
Relative Luciference intensity
Scramble
miR-338-3p
hTERT 3'UTR-WT
hTERT 3'UTR-mut
D
SW1990
E
Relative hTERT mRNA expression (Normolized to GAPDH)
F
Relative miR-338-3p expression(ΔCt)
n=60
P<0.01
Normal
Tumor
G
Relative hTERT expression(ΔCt)
H
r=-0.3358
P=0.0087

Figure 6. miR-338-3p targeted hTERT. A. The target genes of miR-338-3p were analyzed by 5 bioinformatics analysis tools. B. Sequence of miR-338-3p and hTERT 3'-UTR. C and D. The luciferase reporter assay was utilized to monitor the relationship miR-338-3p and hTERT in PC cells. E. The expression change of hTERT in PC cells treated with miR-338-3p mimics. F. Relative miR-338-3p expression in normal and PC tissues. G. hTERT expression in normal and PC tissues (N = 60). H. Correlation of miR-338-3p and hTERT expression in PC tissues ($P = 0.0087$, $r = 0.3358$). $^{**}P < 0.01$.

Table 3. Analysis of the relationship between miR-338-3p and clinical characters in PC

Clinicopathologic Characteristics	No. of patients	miR-338-3p		*P* value
		High	Low	
Age (year)				
> 50	31	16 (51.6%)	15 (48.4%)	0.500
≤ 50	29	14 (48.3%)	15 (51.7%)	
Gender				
Male	33	15 (45.5%)	18 (55.5%)	0.137
Female	27	17 (63.0%)	10 (37.0%)	
Tumor size (cm)				
< 2	28	19 (67.9%)	9 (32.1%)	0.010*
≥ 2	32	11 (34.4%)	21 (65.6%)	
Differentiation grade				
Well/moderately	35	24 (68.6%)	11 (31.4%)	0.005**
Poorly/undifferentiated	25	8 (32.0%)	17 (68.0%)	
Distal metastasis				
M0	24	17 (70.8%)	7 (29.2%)	0.005**
M1	36	12 (33.3%)	24 (66.7%)	
TNM stage				
0 & I & II	20	13 (65.0%)	7 (35.0%)	0.006**
III & IV	40	11 (27.5%)	29 (72.5%)	

$^{*}P < 0.05$, $^{**}P < 0.01$.

(**Figure 6A** and **6B**) because in our previous study, we demonstrated that PCDH10 could impair telomere elongation by suppressing telomerase activity without influencing hTERT expression at the mRNA or protein level. Next, we inserted the hTERT 3'-UTR fragment into the pGL3 vector to generate hTERT 3'UTR-WT and hTERT 3'UTR-Mut. The results signified that miR-338-3p significantly reduced the luciferase activity of hTERT in hTERT 3'UTR-WT group, but not hTERT 3'UTR-Mut group in PaCa-2 and SW1990 cells ($P < 0.01$, **Figure 6C** and **6D**). Moreover, miR-338-3p significantly decreased hTERT expression in PC cells ($P < 0.01$, **Figure 6E**). In addition, we monitored miR-338-3p and hTERT expressions in 60 pairs of normal and PC tissue samples, and miR-338-3p showed a significant downregulation ($P < 0.01$, **Figure 6F**). Moreover, we testified that miR-338-3p expression was relevant to tumor size ($P = 0.010$), differentiation grade ($P = 0.005$), distal metastasis ($P = 0.005$), and tumor, node, metastasis (TNM) stage ($P = 0.006$) but was not related to age ($P = 0.500$) or gender ($P = 0.137$ **Table 3**). Our results also manifested that hTERT expression was remarkably upregulated in PC samples versus normal samples ($P < 0.01$, **Figure 6G**), and miR-338-3p and hTERT expressions exhibited a negative correlation in PC ($P < 0.01$, **Figure 6H**).

miR-338-3p inhibitors and hTERT overexpression reversed the effects of si-circPCDH10 on PC cells

To determine whether circPCDH10 could regulate the progression of PC via hTERT by miR-338-3p, we evaluated the effects of miR-338-3p inhibitors and hTERT on the functions in circPCDH10-silenced PC cells. The downregulation of miR-338-3p induced by si-circPCDH10 in PC cells was weakened by miR-338-3p inhibitors and hTERT ($P < 0.01$, **Figure 7A**). Similarly, si-circPCDH10 significantly reduced hTERT expression in PC cells, which was then blunted by miR-338-3p inhibitors and hTERT ($P < 0.01$, **Figure 7B**). The inhibitory effects of circPCDH10 knockdown on the viability, proliferation, invasion, and migration (shown in **Figure 4**) of PC cells were significantly blocked by the application of miR-338-3p and hTERT ($P < 0.01$, **Figure 7C-F**).

Discussion

It is well documented that circRNAs are generally expressed in cells and extremely conserved, which increases the complexity of the eukaryotic regulatory network [19]. Current research has disclosed that circRNAs can function through diversified ways [26]. Based on the

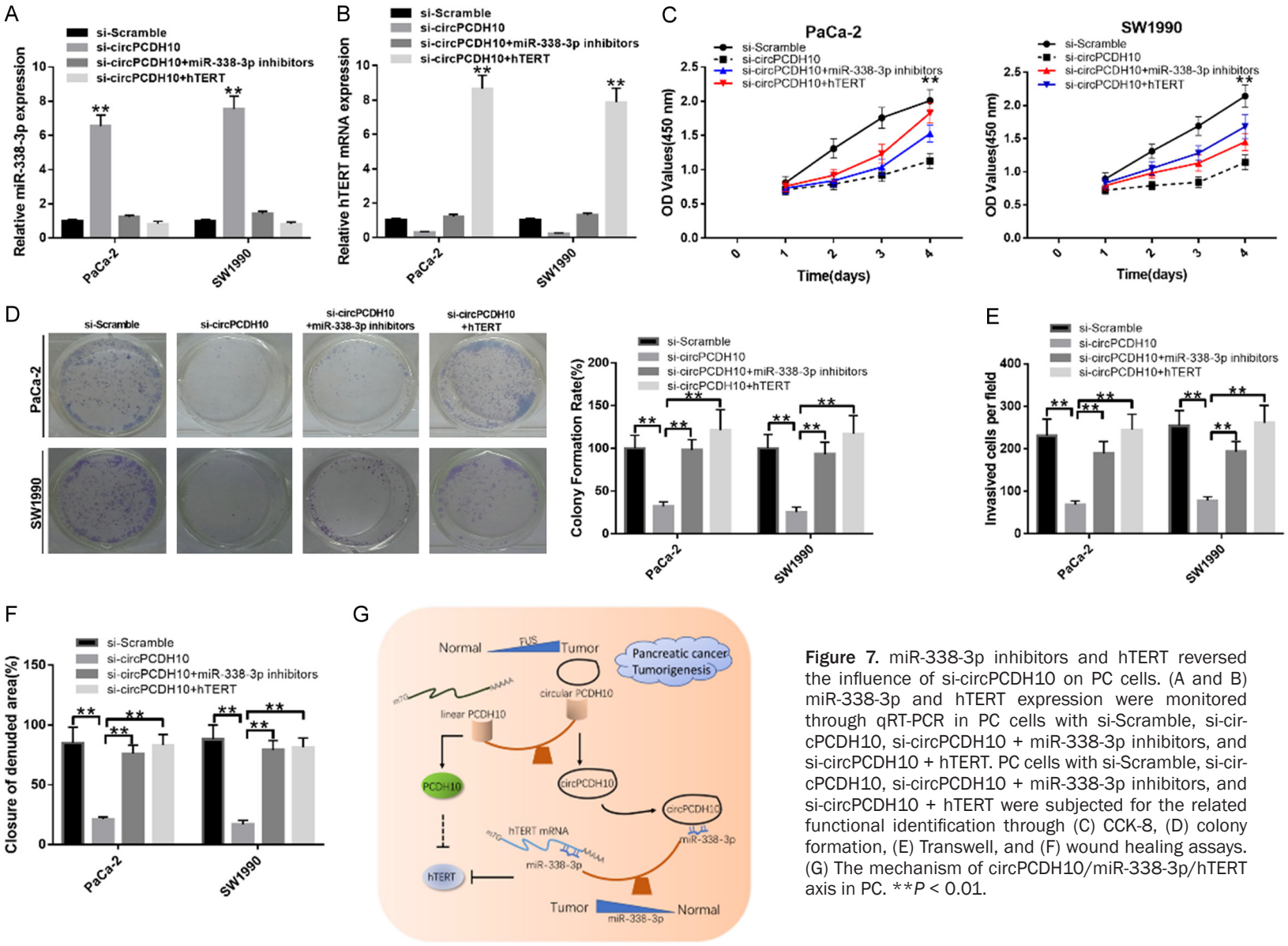

Figure 7. miR-338-3p inhibitors and hTERT reversed the influence of si-circPCDH10 on PC cells. (A and B) miR-338-3p and hTERT expression were monitored through qRT-PCR in PC cells with si-Scramble, si-circPCDH10, si-circPCDH10 + miR-338-3p inhibitors, and si-circPCDH10 + hTERT. PC cells with si-Scramble, si-circPCDH10, si-circPCDH10 + miR-338-3p inhibitors, and si-circPCDH10 + hTERT were subjected for the related functional identification through (C) CCK-8, (D) colony formation, (E) Transwell, and (F) wound healing assays. (G) The mechanism of circPCDH10/miR-338-3p/hTERT axis in PC. $^{**}P < 0.01$.

circBase database, we discovered that circPCDH10 (hsa_circ_0125344) is formed from PCDH10 gene and located in chr4:134075461-134084437, and the spliced sequence length is 472 bp, the best transcript is ENST00000264360.4. According to the literature, we discovered that there was no report on hsa_circ_0125344 (circPCDH10). In our study, we found that the gene encoded by PCDH10 is composed of five exons, among which exons 2-4 can splice into circRNAs. Meanwhile, we proved that originating from the PCDH10 gene but not linear PCDH10, and both PCDH10 linear mRNA and circPCDH10 were present in PC tissues, and circPCDH10 was more stable than PCDH10 linear mRNA in PC.

FUS is widely expressed in human tissues and well demonstrated to function as a regulator in multiple RNA metabolic pathways, including transcription modulation, pre-mRNA splicing, and miRNA processing [27]. In addition, dysregulated FUS expression has been identified in various cancers [11, 13, 28]. However, the underlying molecular mechanisms by which FUS can change the expression level of circRNAs in cancer progression remain largely undetermined. Study also reported that FUS could affect circRNA biogenesis by directly binding to the intron sequences flanking the back-splicing junctions [27]. In accordance with the TCGA database and Kaplan-Meier survival analysis, FUS-downregulated PC patients has a worse survival rate than those FUS-upregulated. Moreover, our data testified that increased FUS in PC cells could induce the formation of circPCDH10, which was circularized by exon 2-4 in the PCDH10 gene by directly binding the PCDH10 pre-mRNA. These results provide additional solid evidence that FUS could negatively regulated the expression of circPCDH10 through binding the introns flanking the circularized exons in PC.

At present, circRNAs have been provecn to significantly influence the biological characteristics of PC cells, such as circZMYM2 [29], circ_100782 [30], circPDE8A [31], circRHOT1 [32], and circ-LDLRAD3. In our study, we first confirmed that circPCDH10 was highly expressed in PC tissues and cells, and high expression of circPCDH10 predicted a poor prognosis in PC. Besides, we certified that knockdown of circPCDH10 could suppress viability and and metastasis of PC cells, and also prevent tumor growth *in vivo*. CircRNAs, with a continuous closed loop structure, can exert biological effects through different regulatory modes [23]. In particular, circRNAs can function as miRNAs molecular sponges or ceRNAs to regulate the translation of target mRNA [33, 34].

In a previous study, the data demonstrated that PCDH10 could reduce the activity of telomerase in PC cells by binding hTERT without influencing hTERT expression at the mRNA or protein level, resulting in the suppression of PC progression [9]. Based on the results of this study, we further speculated whether circPCDH10 could regulate hTERT through certain molecule in PC. MiRNAs, can the growth, proliferation, metastasis and other biological processes of cancer cells through directly or indirectly regulating the target proteins [35, 36]. In this study, through bioinformatics prediction, we also found a novel mechanism by which circPCDH10 can be involved in the regulation of hTERT by sponging miR-338-3p. After a series of experimental verification, we manifested that circPCDH10 could bind to miR-338-3p, and hTERT also was a target gene of miR-338-3p. More importantly, we found that the inhibitory effects of circPCDH10 knockdown on development process of PC could be notably reversed by miR-338-3p inhibition and hTERT overexpression, suggesting the significance of circPCDH10/miR-338-3p/hTERT axis in PC. Of note, the ceRNA regulatory mechanism has limitations. In future studies, we will further explore additional signaling pathways involved in the role of PCDH10 in PC tumorigenesis.

Conclusion

Our findings suggested that increased FUS expression in PC made circPCDH10 the preferred product of the PCDH10 gene, and circPCDH10 might promote PC progression through upregulation of hTERT mediated by miR-338-3p (**Figure 7G**).

Disclosure of conflict of interest

None.

Address correspondence to: Tao Tian, Department of Oncology, Zaozhuang Municipal Hospital, No. 41, Longtou Road, Central District, Zaozhuang 277000, Shandong Province, China. Tel: +86-0632-3288020; Fax: +86-0632-3288020; E-mail: zln1979619@qq.com

References

[1] Kamisawa T, Wood LD, Itoi T and Takaori K. Pancreatic cancer. Lancet 2016; 388: 73-85.

[2] Ilic M and Ilic I. Epidemiology of pancreatic cancer. World J Gastroenterol 2016; 22: 9694-9705.

[3] Mohammed S, Van Buren G 2nd and Fisher WE. Pancreatic cancer: advances in treatment. World J Gastroenterol 2014; 20: 9354-9360.

[4] Zhong X, Shen H, Mao J, Zhang J and Han W. Epigenetic silencing of protocadherin 10 in colorectal cancer. Oncol Lett 2017; 13: 2449-2453.

[5] Liu W, Wu J, Shi G, Yue X, Liu D and Zhang Q. Aberrant promoter methylation of PCDH10 as a potential diagnostic and prognostic biomarker for patients with breast cancer. Oncol Lett 2018; 16: 4462-4470.

[6] Pimson C, Ekalaksananan T, Pientong C, Promthet S, Putthanachote N, Suwanrungruang K and Wiangnon S. Aberrant methylation of PCDH10 and RASSF1A genes in blood samples for non-invasive diagnosis and prognostic assessment of gastric cancer. PeerJ 2016; 4: e2112.

[7] Curia MC, Fantini F, Lattanzio R, Tavano F, Di Mola F, Piantelli M, Battista P, Di Sebastiano P and Cama A. High methylation levels of PCDH10 predict poor prognosis in patients with pancreatic ductal adenocarcinoma. BMC Cancer 2019; 19: 452.

[8] Qiu C, Bu X, Hu D and Jiang Z. Protocadherin 10 (PCDH10) inhibits the proliferation, invasion and migration ability of BXPC-3 pancreatic cancer cells. Xi Bao Yu Fen Zi Mian Yi Xue Za Zhi 2016; 32: 163-167.

[9] Zhou LN, Hua X, Deng WQ, Wu QN, Mei H and Chen B. PCDH10 interacts with hTERT and negatively regulates telomerase activity. Medicine (Baltimore) 2015; 94: e2230.

[10] Harrison AF and Shorter J. RNA-binding proteins with prion-like domains in health and disease. Biochem J 2017; 474: 1417-1438.

[11] Ghanbarpanah E, Kohanpour MA, Hosseini-Beheshti F, Yari L and Keshvari M. Structure and function of FUS gene in prostate cancer. Bratisl Lek Listy 2018; 119: 660-663.

[12] Feng Y, Yang Y, Zhao X, Fan Y, Zhou L, Rong J and Yu Y. Circular RNA circ0005276 promotes the proliferation and migration of prostate cancer cells by interacting with FUS to transcriptionally activate XIAP. Cell Death Dis 2019; 10: 792.

[13] Zhu H, Zheng T, Yu J, Zhou L and Wang L. LncRNA XIST accelerates cervical cancer progression via upregulating Fus through competitively binding with miR-200a. Biomed Pharmacother 2018; 105: 789-797.

[14] Bian S. miR-4319 inhibited the development of thyroid cancer by modulating FUS-stabilized SMURF1. J Cell Biochem 2020; 121: 174-182.

[15] He Z, Ruan X, Liu X, Zheng J, Liu Y, Liu L, Ma J, Shao L, Wang D, Shen S, Yang C and Xue Y. FUS/circ_002136/miR-138-5p/SOX13 feedback loop regulates angiogenesis in Glioma. J Exp Clin Cancer Res 2019; 38: 65.

[16] Guo Q, Jiang LX and Hu B. Cell apoptosis and proliferation inhibition of pancreatic cancer induced by sub-threshold focused ultrasound (FUS). Eur J Radiol 2012; 81: e704-707.

[17] Ashwal-Fluss R, Meyer M, Pamudurti NR, Ivanov A, Bartok O, Hanan M, Evantal N, Memczak S, Rajewsky N and Kadener S. circRNA biogenesis competes with pre-mRNA splicing. Mol Cell 2014; 56: 55-66.

[18] Conn SJ, Pillman KA, Toubia J, Conn VM, Salmanidis M, Phillips CA, Roslan S, Schreiber AW, Gregory PA and Goodall GJ. The RNA binding protein quaking regulates formation of circRNAs. Cell 2015; 160: 1125-1134.

[19] Ebbesen KK, Kjems J and Hansen TB. Circular RNAs: identification, biogenesis and function. Biochim Biophys Acta 2016; 1859: 163-168.

[20] Shanmugapriya, Huda HA, Vijayarathna S, Oon CE, Chen Y, Kanwar JR, Ng ML and Sasidharan S. Functional analysis of circular RNAs. Adv Exp Med Biol 2018; 1087: 95-105.

[21] He J, Xie Q, Xu H, Li J and Li Y. Circular RNAs and cancer. Cancer Lett 2017; 396: 138-144.

[22] Das A, Gorospe M and Panda AC. The coding potential of circRNAs. Aging (Albany NY) 2018; 10: 2228-2229.

[23] Patop IL and Kadener S. circRNAs in cancer. Curr Opin Genet Dev 2018; 48: 121-127.

[24] An N and Cheng D. The long noncoding RNA HOST2 promotes gemcitabine resistance in Human pancreatic cancer cells. Pathol Oncol Res 2018; 26: 425-431.

[25] Li J, Li Z, Jiang P, Peng M, Zhang X, Chen K, Liu H, Bi H, Liu X and Li X. Circular RNA IARS (circ-IARS) secreted by pancreatic cancer cells and located within exosomes regulates endothelial monolayer permeability to promote tumor metastasis. J Exp Clin Cancer Res 2018; 37: 177.

[26] Geng Y, Jiang J and Wu C. Function and clinical significance of circRNAs in solid tumors. J Hematol Oncol 2018; 11: 98.

[27] Errichelli L, Dini Modigliani S, Laneve P, Colantoni A, Legnini I, Capauto D, Rosa A, De Santis R, Scarfo R, Peruzzi G, Lu L, Caffarelli E, Shneider NA, Morlando M and Bozzoni I. FUS affects circular RNA expression in murine embryonic stem cell-derived motor neurons. Nat Commun 2017; 8: 14741.

[28] Xiong D, Wu YB, Jin C, Li JJ, Gu J, Liao YF, Long X, Zhu SQ, Wu HB, Xu JJ and Ding JY. Elevated FUS/TLS expression is negatively associated

with E-cadherin expression and prognosis of patients with non-small cell lung cancer. Oncol Lett 2018; 16: 1791-1800.
[29] An Y, Cai H, Zhang Y, Liu S, Duan Y, Sun D, Chen X and He X. circZMYM2 competed endogenously with miR-335-5p to regulate JMJD2C in pancreatic cancer. Cell Physiol Biochem 2018; 51: 2224-2236.
[30] Chen G, Shi Y, Zhang Y and Sun J. CircRNA_100782 regulates pancreatic carcinoma proliferation through the IL6-STAT3 pathway. Onco Targets Ther 2017; 10: 5783-5794.
[31] Li Z, Yanfang W, Li J, Jiang P, Peng T, Chen K, Zhao X, Zhang Y, Zhen P, Zhu J and Li X. Tumor-released exosomal circular RNA PDE8A promotes invasive growth via the miR-338/MACC1/MET pathway in pancreatic cancer. Cancer Lett 2018; 432: 237-250.
[32] Qu S, Hao X, Song W, Niu K, Yang X, Zhang X, Shang R, Wang Q, Li H and Liu Z. Circular RNA circRHOT1 is upregulated and promotes cell proliferation and invasion in pancreatic cancer. Epigenomics 2019; 11: 53-63.
[33] Louis C, Desoteux M and Coulouarn C. Exosomal circRNAs: new players in the field of cholangiocarcinoma. Clin Sci (Lond) 2019; 133: 2239-2244.
[34] Xiong DD, Dang YW, Lin P, Wen DY, He RQ, Luo DZ, Feng ZB and Chen G. A circRNA-miRNA-mRNA network identification for exploring underlying pathogenesis and therapy strategy of hepatocellular carcinoma. J Transl Med 2018; 16: 220.
[35] Deb B, Uddin A and Chakraborty S. miRNAs and ovarian cancer: an overview. J Cell Physiol 2018; 233: 3846-3854.
[36] Tutar L, Özgür A and Tutar Y. Involvement of miRNAs and pseudogenes in cancer. Methods Mol Biol 2018; 1699: 45-66.